Indian Journal of Geo Marine Sciences
Vol. 50 (07), July 2021, pp. 521-532

Evolution mechanism of contrasting phases of consecutive IOD events from 1994 to 1998

N Anil*[,a], M R Ramesh Kumar[b], R Sajeev[a] & P K Saji[a]

[a]Department of Physical Oceanography, Cochin University of Science and Technology, Kochi, Kerala – 682 016, India
[b]Physical Oceanography Division, National Institute of Oceanography, Dona Paula, Goa – 403 004, India

*[E-mail: nisaanil1111@gmail.com]

Received 27 January 2021; revised 25 May 2021

The Dipole Mode Index (DMI), an Index used to represent the Indian Ocean Dipole (IOD), shows a back to back occurrence of positive and negative IOD events during the period 1994 to 1998. The year 1994 was a strong positive IOD year and was followed by a strong negative IOD in 1996. The positive IOD in 1997 and negative IOD in 1998 were co-occurred with the strong El-Nino and strong La-Nina, respectively. In the present study, we have looked into the evolution of consecutive IOD events during the period 1994 to 1998 and analyzed the differences in their formation, features and association with Indian Summer Monsoon Rainfall (ISMR) for various homogenous regions of the Indian subcontinent. We have found that the El-Nino and La-Nina enhances the IOD-induced positive SST anomalies in the western and eastern parts of the Indian Ocean during the co-occurred years, respectively. The evolution of positive IOD in 1997 is driven by the strong easterly wind anomalies associated with strong El-Nino. The positive anomalies of SST in the western equatorial Indian Ocean is maintained by the El-Nino which results in the long life span of positive IOD in the year 1997 than that of pure positive IOD year 1994. The westward propagating Rossby wave generated due to PIOD is maintained by strong El-Nino in the year 1997. The vertical dynamics, represented by D20, showed minor differences during the pure and co-occurred IOD events. The positive IOD years with El-Nino had good correlation with the Peninsular India and Central North East India regions rainfall. Since we have used only limited samples or cases under the different categories, our present results are preliminary in nature.

[Keywords: Ekman transport, El-Nino, Indian Ocean, Indian Ocean Dipole, La-Nina, Monsoon]

Introduction

Unlike other tropical oceans, Indian Ocean is featured with a warm Sea Surface Temperature (SST) on the eastern equatorial Indian Ocean (IO) and a cooler SST at the west. However, in some years, the Equatorial Indian Ocean (EIO) becomes cooler at the east and warmer at the west. This irregular oscillations in SST in which the western IO becomes warmer and the eastern IO becomes cooler is termed as Indian Ocean Dipole (IOD)[1,2]. It is one of the important forcing for the inter-annual variability of Indian Ocean basin. This feature, which is irregular in nature, consists of positive and negative phases. The intensity of the oscillation is represented by an index called Dipole Mode Index (DMI), which is defined as the difference in SST Anomaly (SSTA) of west (50° E – 70° E; 10° S – 10° N) and east (90° E – 110° E; -10° S – EQ) in the equatorial Indian Ocean[1]. A positive (negative) IOD is characterized with a positive (negative) DMI index having negative (positive) SST anomaly at east and positive (negative) SST anomaly at west.

There are discrepancies in the definition as well as in the evolution of this interannual phenomenon. Earlier IOD was believed to be developed as a consequence of El-Nino forcing from the Pacific[3]. But later, it was found that IOD develops during non-El Nino years[4] and concludes that El-Nino is not essential for the formation of an IOD[5]. Thermocline shoaling and enhanced evaporation prior to the onset of IOD in the southeastern Indian Ocean shows the importance of subsurface forcing on IOD formation[6].

An understanding of the formation and evolution of the contrasting phases of IOD phenomena is essential to estimate its impacts on the climate of Indian Ocean and its surrounding countries. A positive IOD can suppress the negative effect of El-Nino and contribute average to above average rainfall over the Indian subcontinent[7]. On the other hand, the combined effect of IOD and El-Nino brings a reduced rainfall over

Australia[8,9]. The number of positive IOD years has increased during the past few decades that include a hatric of events in 2006, 2007 and 2008, which had resulted in the prolonged drought conditions over the eastern part of Australia[10]. A recent study explains the severity of two consecutive positive IOD events of 2019/2020 on Australian bush fires[11].

Vinayachandran *et al.*[4], showed that the strong positive IOD event in 1994 had unusual easterlies in the eastern equatorial Indian Ocean, which persisted for about eight months (April-November). Further, the year 1994 was also identified as an anomalous year with unusual cooling of the southeastern equatorial Indian Ocean[12]. A recent study by Saji *et al.*[13], pointed out the strong influence of the positive dipole event in 1994 driving the equatorial Pacific Ocean surface characteristics.

The negative IOD event is associated with a cooler SSTA in the west and a warmer SSTA over the east. The higher evaporation rates over Eastern Box (EB) during this period contribute to incessant rainfall over southeastern parts of Australia and drought conditions in western Indian Ocean and east Africa. Incidentally, Bureau of Meteorology, Australia also reported the year 1996 as the second warmest winter ever.

The year 1997, when IOD and El-Nino was co-occurred, is characterized as a strongest El-Nino event in the history. This El-Nino is categorized as super El-Nino by Saji *et al.*[13] because of its different characteristics and impacts as compared to other El-Nino events. This may have an effect on the evolution and features of IOD co-occurred during the same time. The termination of 1997 El-Nino is happened in mid-1998 which was followed by a strong La-Nina that was co-occurred with the negative IOD in the Indian Ocean. The 1998 La-Nina had a two year life span (up to year 2000) and is unique in characteristics with the canonical La-Nina years[14].

Hong *et al.*[15] studied the difference in the evolution and spatial characteristics of IODs with and without El-Nino Southern Oscillation (ENSO) (1948-2002). They have discussed the variations in the air-sea parameters during the evolution of IOD and its influence on Asian rainfall.

As different from previous studies, we examine the evolution of consecutive occurrence of contrasting IOD events from 1994 to 1998. The years 1994 and 1996 are characterized with strong positive and negative IODs, respectively. The year 1995 was a transition period from positive to negative IOD. The year 1996 was then followed by a strong positive IOD year and co-occurred with the strongest El-Nino of the century in 1997, which was again transited to a strong negative IOD year co-occurred with a strong La-Nina event in 1998. The IODs in 1994 and 1996 are considered as pure IOD events (independent of El-Nino) and that in 1997 and 1998 are co-occurred events with El-Nino Southern Oscillation (ENSO). Also we looked in to the role of IOD events with and without ENSO on Indian Summer Monsoon Rainfall over 5 homogeneous regions *viz*. Northwest India, Central Northeast India, Northeast India, West Central India & Peninsular India[16].

This paper was motivated by the lack of clarity in the formation mechanism of IOD events. This paper has examined the evolution of the different phases of strong IOD events, during consecutive years from 1994 to 1998. Emphasis was also given to reveal the influence of each IOD event, with and without ENSO, on the variability of summer monsoon rainfall at five meteorological regions of Indian subcontinent.

Materials and Methods

A suite of data sets has been used in this study which includes satellite and re-analysis data products. The DMI data was obtained from Japanese Agency for Marine-Earth Science Technology (JAMSTEC) website. The El-Nino and La-Nina years are taken from the Golden Gate Weather Services (https://ggweather.com/enso/oni.htm) website. The rainfall data over India and 5 homogenous regions of Indian subcontinent have been extracted for the study period (1960 to 2016) from the study of Kothawale & Rajeevan[16]. Further, the same homogenous regions as used by Kothawale & Rajeevan[16] were used in the present study. The years of positive IOD, positive IOD & El-Nino co-occurred event, negative IOD, negative IOD & La-Nina co-occurred events are listed in Table 1.

The IOD years are taken from Bureau of Meteorology (http://www.bom.gov.au/climate/iod/) website. The ocean-atmospheric parameters such as

Table 1 — The years of positive IOD, positive IOD & El-Nino co-occurred event, negative IOD, negative IOD & La-Nina co-occurred events

Pure Positive IOD	Positive IOD + El-Nino	Negative IOD	Negative IOD + La-nina
1961	1972	1960	1964
1963	1982	1981	1974
1967	1997	1989	1998
1983	2006	1992	2010
1994	2015	1996	2016
2012		2014	

SST, wind speed, Latent Heat Flux (LHF) and Net Heat Flux (NHF) were extracted from TropFlux data sets[17]. The Hamburg Ocean Atmosphere Parameters and Fluxes from Satellite (HOAPS) data was used for the analysis of monthly rainfall[18]. The sub-surface temperature data was taken from Simple Ocean Data Assimilation (SODA V2.2.4)[19] to estimate the depth of isotherms (20 and 26 °C). The wind data from European Remote Sensing Satellite (ERS-2)[20] was used for computing Ekman transport using the formula,

$$Mxe = \tau_y / f \quad \ldots (1)$$

Where, τ_y is the meridional wind stress and f is the Coriolis parameter defined as,

$$\tau_y = \rho_a C_D w v \quad \ldots (2)$$

and

$$f = 2 \Omega \sin\Phi \quad \ldots (3)$$

Where, ρ_a is the air density, C_D is the drag coefficient, w is the mean wind speed, v is the meridional wind component, Ω is the angular velocity of the Earth and Φ is the latitude.

In order to study the evolution of IODs from 1994 to 1998, the life period of an IOD was categorized into four phases such as onset, developing, mature and termination phase.

Results and Discussion

From the monthly DMI (Fig. 1), it can be seen that strong IOD events with positive and negative phases are occurred during the period 1994 to 1998 with a transitional/neutral year of 1995. The years 1994 and 1996 are positive and negative IOD years, respectively; followed by years of positive IOD co-occurred with the super El-Nino in 1997 and a negative IOD with strong La-Nina in 1998.

There have been several hypotheses regarding the evolution of IOD events (for example, Ueda & Matsumoto[21]; Kajikawa *et al.*[22]). In general, the generation of an IOD occurs in May – June and terminates by November – December of the same year. In order to delineate the significant features in the evolution of IOD events, the 4 months (June, August, October and December) were selected to represent the phases of evolution (onset, developing, mature and termination) of IOD events, respectively.

Figure 2 shows the composite of monthly DMI for pure (independent) positive IOD (PIOD) years of 1961, 1963, 1977, 1994 and 2012 and the El-Nino-PIOD co-occurred years of 1972, 1982, 1997 and

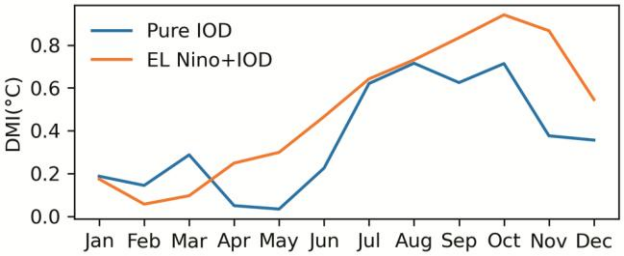

Fig. 2 — The monthly DMI for the composite of pure positive IOD years (1961, 1963, 1967, 1983, 1994 & 2012) and El-Nino-IOD co-occurred events (1972, 1982, 1997, 2006 & 2015)

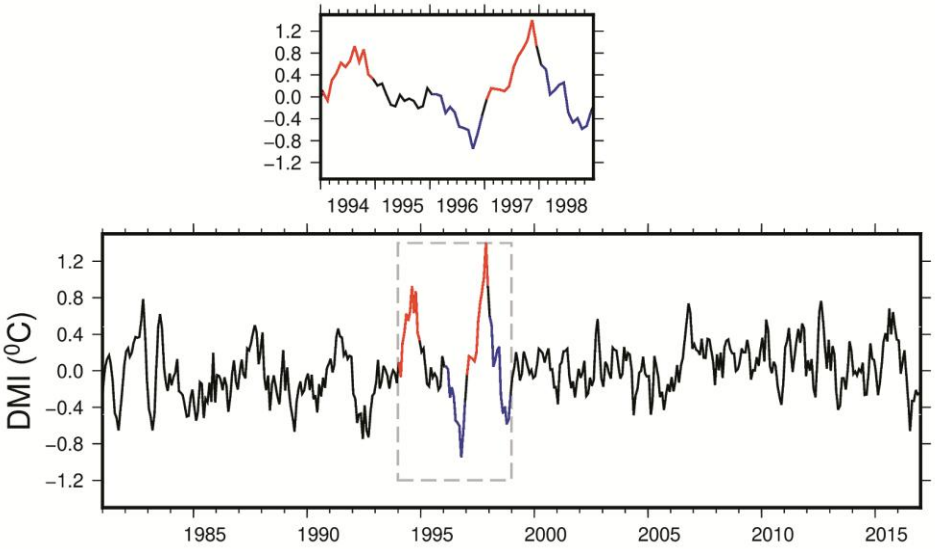

Fig. 1 — The monthly Dipole Mode Index (DMI) for the period from 1981 to 2016 (bottom figure) and the top figure represents the monthly DMI of the study years from 1994 to 1998 separately (blue color represents the positive IODs and red color represents the negative IODs)

2015. In case of co-occurred composite, the intensity of DMI index values are generally high and DMI keeps increasing from the month of February and peaks in October. In contrast, the pure IOD forms in the month of May and shows two peaks, one in August and the other in October. The life span of pure IOD is comparatively lesser than that of the co-occurred years. The DMI values for Negative IOD (NIOD) year and co-occurred year shows an opposite pattern till the month of September. The intensity of pure NIOD year is more than that of NIOD-La-Nina co-occurred year, which peaks in June. The co-occurred event has its peak in October. The pure NIOD is having negative DMI values prior to the onset till termination, which shows it have a long life span by evolving independently. In contrast, the PIOD is having high intensity and long life span during El-Nino and PIOD co-occurred events.

While comparing the DMI for the years 1994 (pure IOD) and 1997 (IOD+El-Nino), the pure IOD event has two peaks, one in August and the other in October like in the composite of the pure PIOD events (Fig. 2). The PIOD in 1994 has high intensity in the onset (June) and developing (August) phases. In the maturing phase, the co-occurred year of 1997 showed high intensity. The intensity at the peak was higher for El-Nino+PIOD year and the maximum value was observed in November. In the case of negative IOD years of 1996 and 1998, the intensity is found to be higher in the case of pure NIOD than the co-occurred year as seen in the composite. The peaking of IOD occurred in October for the year 1996 and in November for 1998 event.

Vinayachandran *et al*.[4] suggested that the southeast wind along the Sumatra coast is considered as a forerunner for a positive IOD. The wind pattern during the onset stage of 1994 event supports this hypothesis. The wind speed anomaly in the EB is having less intensity during 1997 in the onset phase (June), which is reflected in the SST anomaly pattern for the onset (Fig. 3b). The maximum intensity of wind speed anomaly in the EB is seen during the mature phase for both 1994 and 1997 years. The negative SST anomaly in the Eastern Box (EB; Fig. 3f) is highest in August in the case of pure IOD event and was in October in the case of El-Nino and IOD co-occurred year. Hence, El-Nino affects the evolution of IOD by shifting the occurrence of the peak to two months. These negative anomalies are reaching up to the Western Box (WB; Fig. 3f) during the mature phase of 1997 because the strong easterlies extend up to the WB.

The PIOD pattern in the surface SST anomaly diminishes in the termination phase even if the easterlies prevail during 1994 (Fig. 3g). During 1997, the termination phase is showing a strong surface PIOD pattern (Fig. 3h) with high intense easterlies which prove that the super El-Nino in 1997 increased the life span of the PIOD.

In the case of NIOD, the negative anomalies of SST are only visible in the case of pure event throughout the evolution process (Fig. 4). Even if the westerly winds are very much stronger during the mature phase of 1998, the western box is holding a positive SST anomaly. During the co-occurred year of NIOD and La-Nina (1998), the dipole pattern in SST anomaly is significantly maintained by warm water advection from Pacific. The co-occurred events of PIOD and NIOD with El-Nino and La-Nina, contributes warmer SST anomalies into almost all parts of the Indian Ocean.

The offshore mass transport due to strong along shore component of wind is the primary driving force for upwelling in the EB during PIOD years. The meridional transport is visible in the year 1994 from onset phase onwards while the transport is weak in case of 1997 event (Fig. 5a). The intensity of Ekman transport (negative *Mxe values*) becomes maximum during the developing phase and most part of the EB possess positive Mxe values during the termination phase of pure PIOD event (Figs. 5e & g). The Ekman transport is found to be less intense in the co-occurred year 1997 as compared to the pure IOD year. However the absence of easterlies during both NIOD years (1996 as well as 1998) is incapable of producing Ekman transport (Fig. 6) that resulted in the deepening of the thermocline.

Annual cycle of ocean-atmospheric parameters

The annual cycle of various ocean-atmospheric parameters over the EB are presented for the years 1994 and 1997 in Figure 7 and for the years 1996 and 1998 in Figure 8 in order to compare the differences in the evolution of the respective IODs.

The negative SST anomaly in the pure PIOD year was higher from the onset till the mature phase than the PIOD-El-Nino co-occurred year. During the termination in November, 1997 is having higher intensity. But after the mature stage pure IOD suddenly start diminishing. The positive SST anomaly during the NIOD year was found higher in the case of NIOD-La-Nina co-occurred event than that of a pure NIOD year.

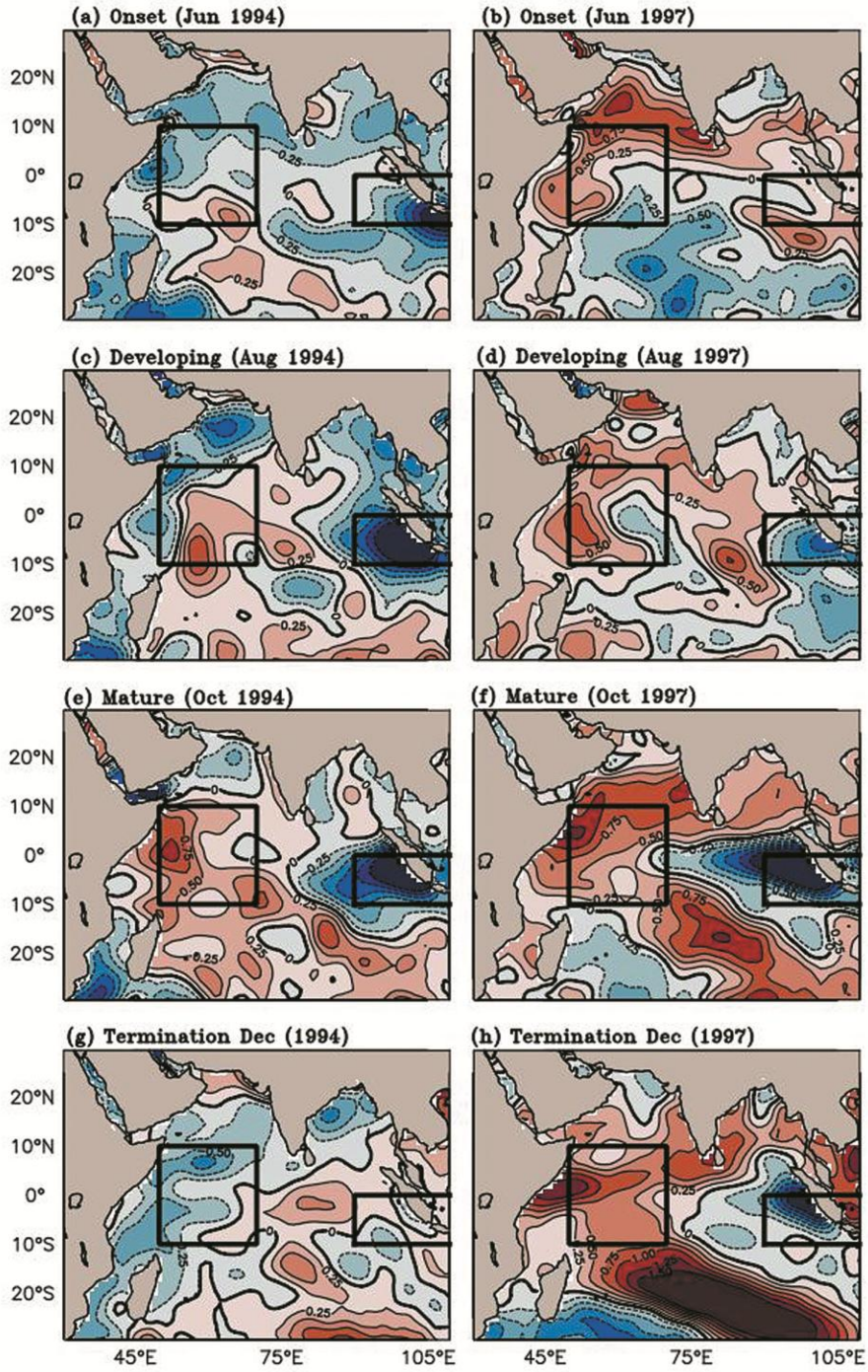

Fig. 3 — SST anomaly for the pure IOD (1994) and El-Nino-IOD co-occurred event (1997) for the different phases of evolution

The wind speed is observed to be higher for the year 1994 than 1997 event during the onset and developing phase which resulting in the high negative anomalies in pure PIOD year in the eastern box. During the matured and termination phase, the intensity is higher for El-Nino-PIOD co-occurred year and that is the reason for high negative SST anomaly seen in the termination phase of 1997 event. Even if the wind speed anomaly is negative in almost all the months, the NIOD-La-Nina co-occurred event possesses a high positive SST anomaly may be because of the Indonesian through flow which carry warmer water from the western Pacific ocean to the eastern equatorial Indian Ocean.

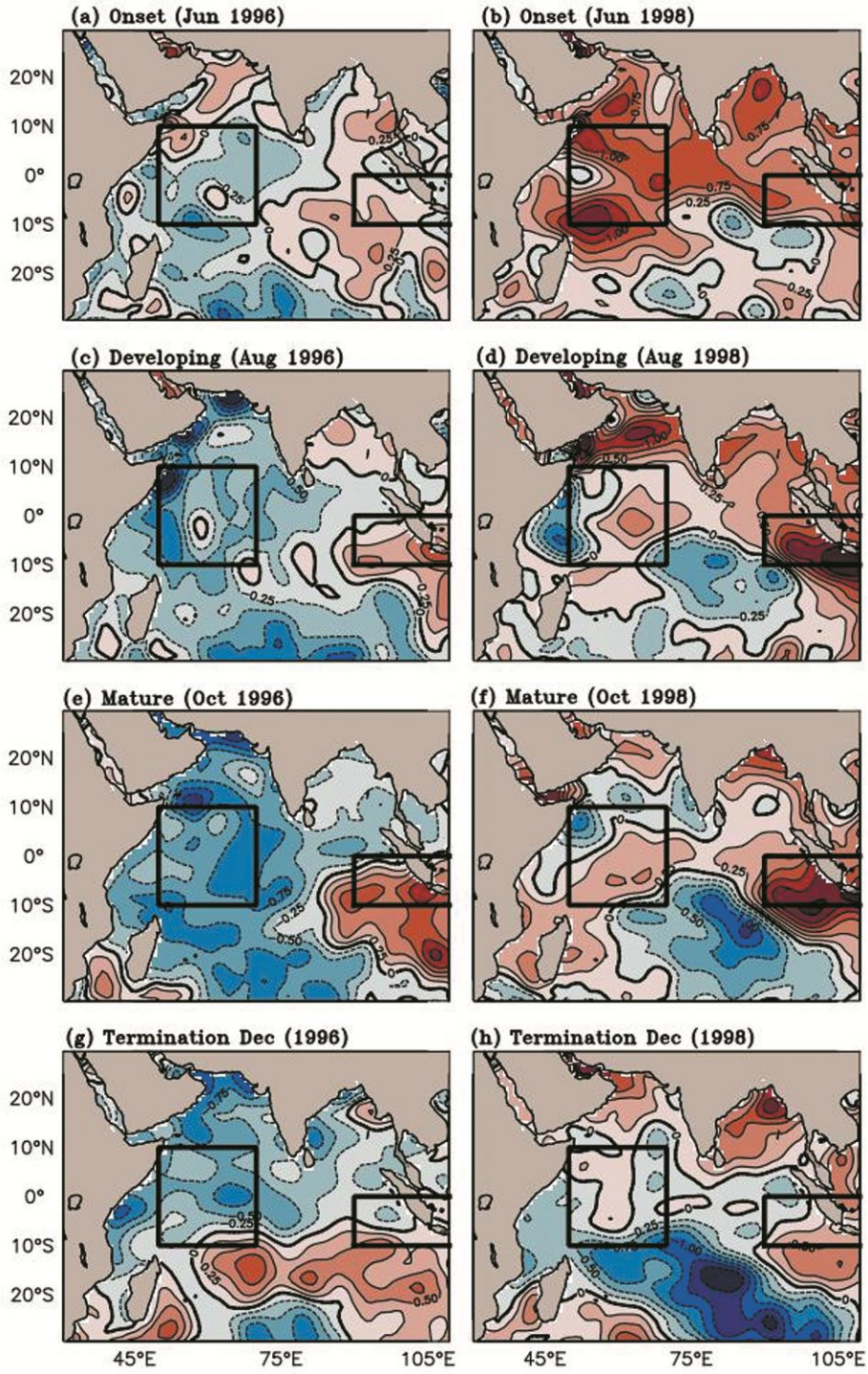

Fig. 4 — SST anomaly for the pure negative IOD (1996) and La-Nina-negative IOD co-occurred event (1998) for the different phases of evolution

The Latent Heat Flux anomaly (LHF) values showed almost similar variability that of wind speed, as they are directly proportional. The increase in wind speed enhances evaporation, which is reflected in the LHF anomaly pattern in 1994 and 1997. It showed a positive value in the onset and developing phase of both 1994 and 1997. In the case of 1996, the LHF possess negative values in almost all the months except in the termination phase. But in case of 1998, the LHF anomalies are positive from the developing

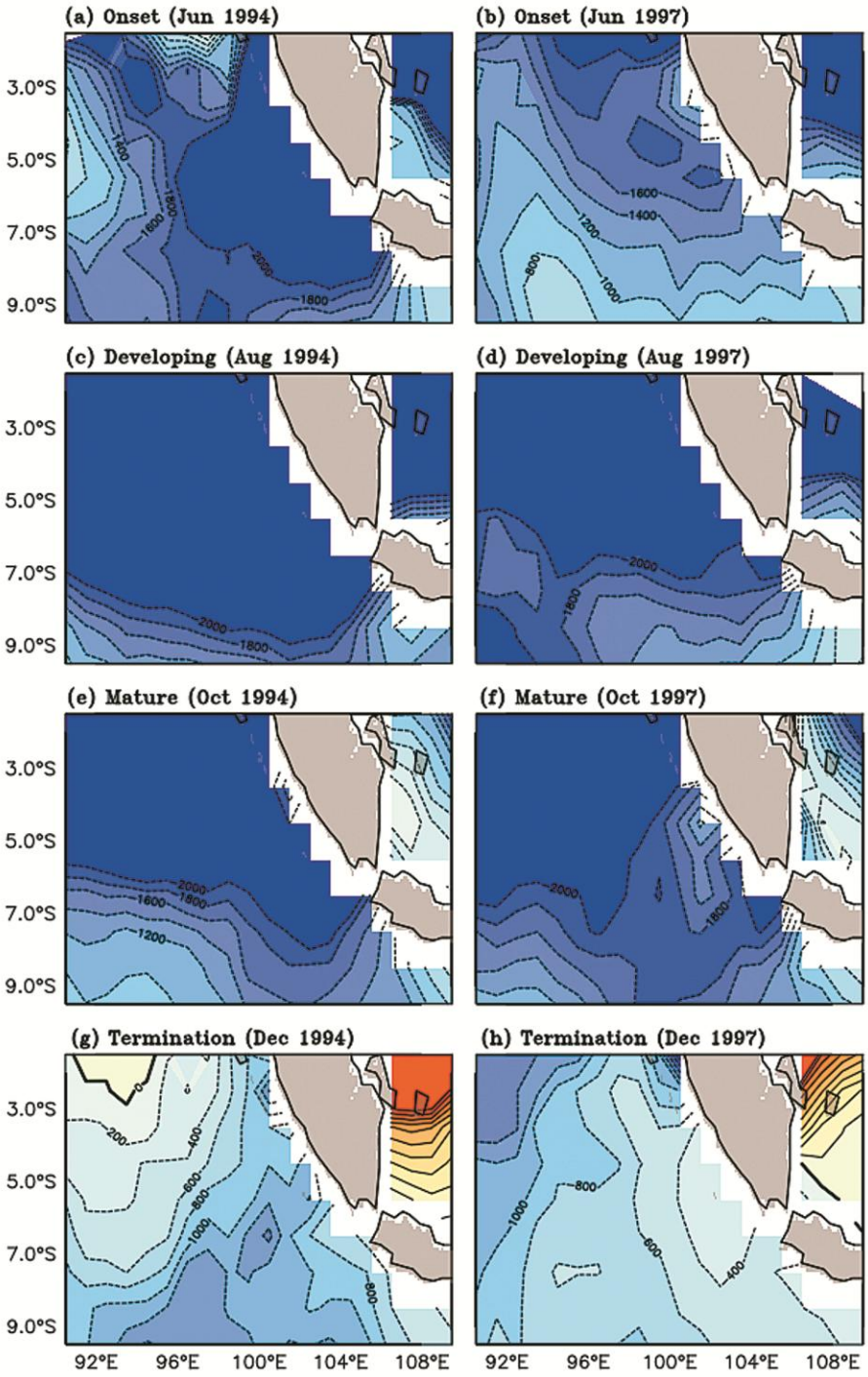

Fig. 5 — Ekman transport (kg m^{-1} s^{-1}) in the eastern box [90E:110E; 10S: EQ] during the pure IOD (1994) and El-Nino-IOD co-occurred event (1997) for the different phases of evolution

stage till termination. It still maintained the SST anomaly positive through horizontal advection of warm water towards the eastern equatorial Indian Ocean.

The Net Heat Flux (NHF) is positive (heat gain by the ocean) in the mature and termination months for both the years of 1994 and 1997. Even if the eastern box is gaining more heat, it could not overcome the effect of vertical advection of cooler subsurface waters on SST during the developing and mature phase of PIOD in both the years. During the termination phase NHF anomalies keep increasing

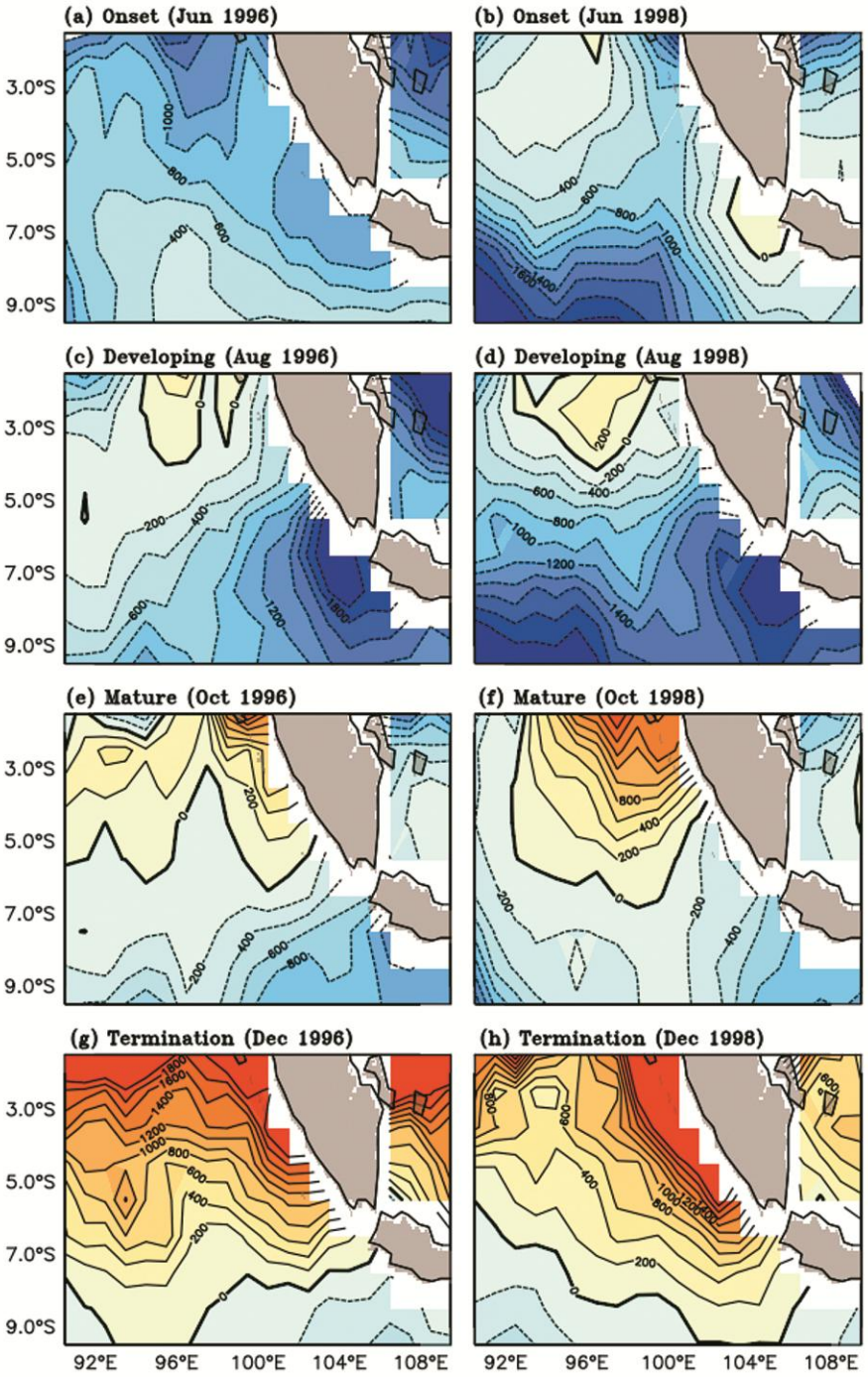

Fig. 6 — Ekman transport (kg m^{-1} s^{-1}) in the eastern box [90E:110E; 10S: EQ] during the pure negative IOD (1996) and La-Nina-negative IOD co-occurred event (1998) for the different phases of evolution

which results in the abrupt termination of surface features of pure IOD event in 1994 during the termination phase (Fig. 3g). But in case of 1997 co-occurred year of PIOD, strong easterlies and positive SST anomalies in western equatorial Indian Ocean, maintains the PIOD pattern (Fig. 3h) as a result of influence of strong El-Nino in 1997. During the events of 1996 and 1998, the NHF is almost negative throughout the year, but it showed a positive SST anomaly because of the horizontal advection from the Pacific.

The rainfall is having low values for both pure PIOD and El-Nino-PIOD co-occurred events because of suppressed convection over the eastern box. It is

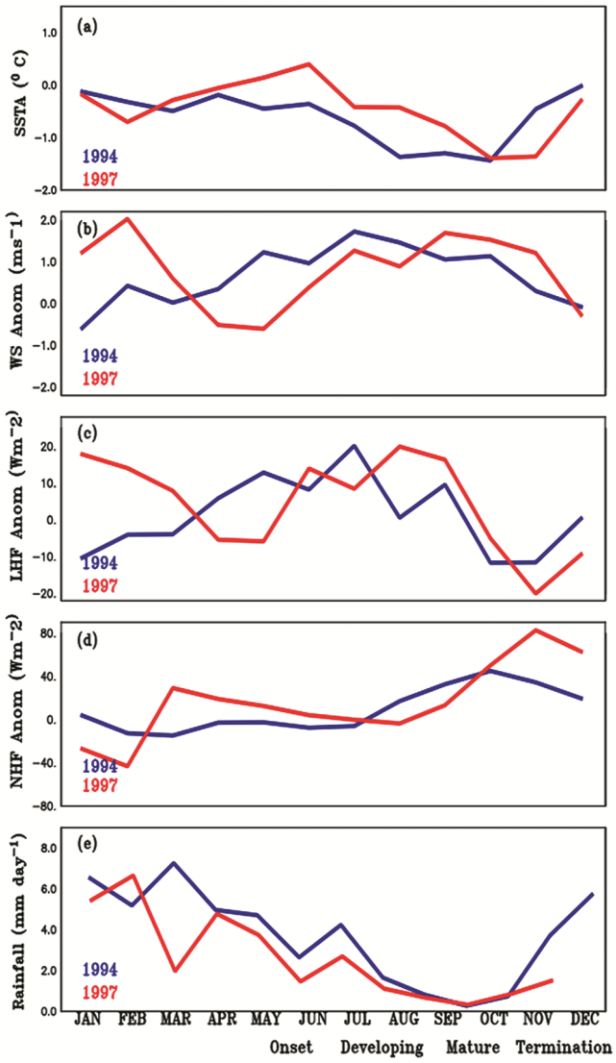

Fig. 7 — Annual cycle of ocean-atmospheric parameters (SST anomaly, wind speed anomaly, LHF anomaly, NHF anomaly and Rainfall) for the pure IOD (1994) and El-Nino-IOD co-occurred event (1997) for the different phases of evolution for the eastern box [90E:110E; 10S: EQ]

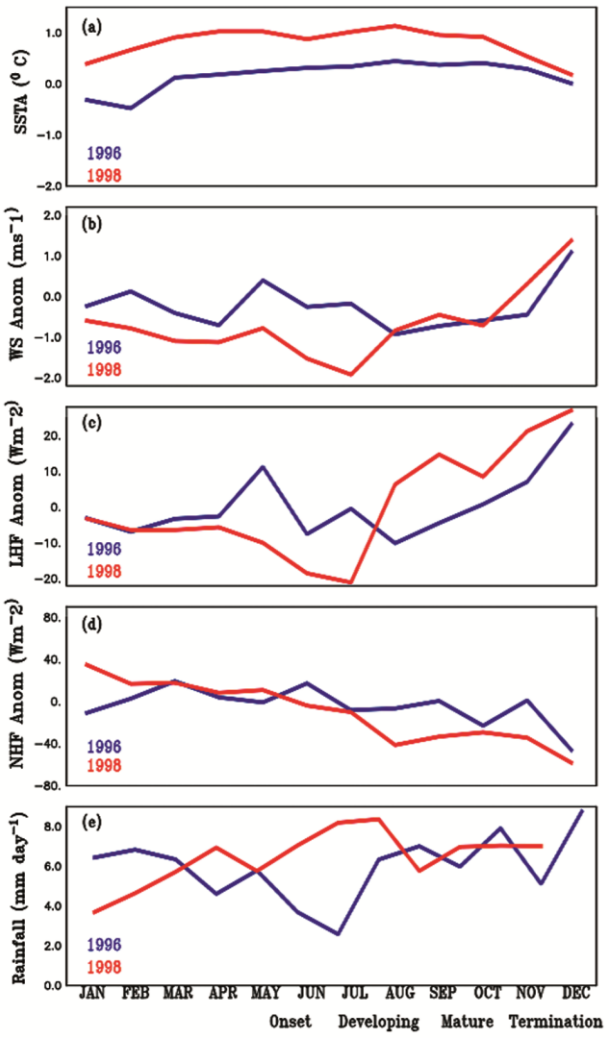

Fig. 8 — Annual cycle of ocean-atmospheric parameters (SST anomaly, wind speed anomaly, LHF anomaly, NHF anomaly and Rainfall) for the pure negative IOD (1996) and La-Nina-negative IOD co-occurred event (1998) for the different phases of evolution for the eastern box [90E:110E; 10S: EQ]

almost zero mm/day during the mature phase of both the events. The case reverses during 1996 and 1998 having a higher rainfall in the eastern box because of enhanced convection. The higher values are seen almost for all months in the NIOD-La-Nina co-occurred event than the pure NIOD event.

The subsurface variability of oceanic parameters during the evolution of events from 1994 to 1998 is demonstrated in Figure 9. The temperature variation in the subsurface is directly linked to the vertical movement of thermocline. The shoaling of thermocline is visible prior to the onset of PIOD in 1994. The negative temperature anomalies are wider than the surface anomalies. Hence the cooler temperature prevails in the subsurface even the surface signals got diminished. During 1997, the subsurface temperature is deeper, cooler and wider than that of 1994 PIOD year. But the surface feature got terminated because of the occurrence of 1998 La-Nina which transmits the warm water over the EB of the Indian Ocean. The pure NIOD possess maximum temperature at 100 m depth during the maturing stage.

To capture the upwelling features, the depth of 20° (D20) and 26° (D26) isotherms are plotted over the time-depth section of the ocean temperature (Fig. 9). It can be seen that, for the pure IOD (year 1994), the maximum value of D20 (98 m) is seen in the matured phase (September) and is lesser (78 m) in the case of El-Nino+IOD (year 1997). This means that the D20

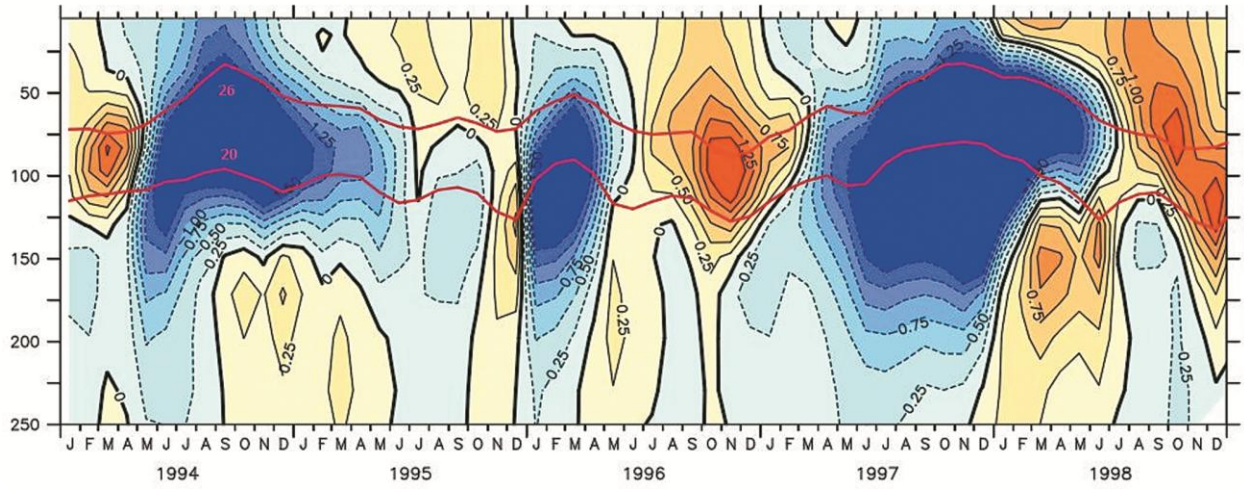

Fig. 9 — Time-depth section of ocean temperature anomaly for eastern box [90E:110E; 10S: EQ] overlaid with 20 °C and 26 °C isotherm

persist with a depth of 78 m for about 4 months in the case of El-Nino-IOD co-occurred event. The D26 showed in-phase variability with that of D20 but with lower (32 m) depth values. The D26 also persists for 4 to 5 months in the year 1997 at almost the same depth. During the pure negative IOD year, the depth of D26 is much similar to that of co-occurred event *i.e.* 84 m. The depth of 20 degree isotherm was higher (132 m) during the co-occurred events than that during the pure events (125 m).

The Hovmoller diagram is plotted for the sea surface height in order to look at the difference in the formation and propagation of Rossby waves during the pure and co-occurred years of IOD. A westward propagating Rossby wave during pure PIOD year 1994 as well as in the co-occurred years of El-Nino-PIOD year 1997 can be seen in the figure (Fig. S1). The strength of the wave is much higher in the case of co-occurred year and had a longer life span. The Rossby wave is maintained till the next year (1998) up to the termination of El-Nino. The strong easterlies during the co-occurred year are responsible for the westward propagation and maintenance of these down-welling Rossby waves. During the pure PIOD year, the easterlies are not having high intensities and it is not reaching up to the western equatorial Indian Ocean; hence the wave propagation is only seen up to the central equatorial Indian Ocean. So, the Rossby wave generated by IOD is maintained by El-Nino in the Pacific Ocean.

The monthly ISMR (June to September) of the five homogenous regions (Northwest India, Central Northeast India, Northeast India, West Central India & Peninsular India India) were analyzed for their

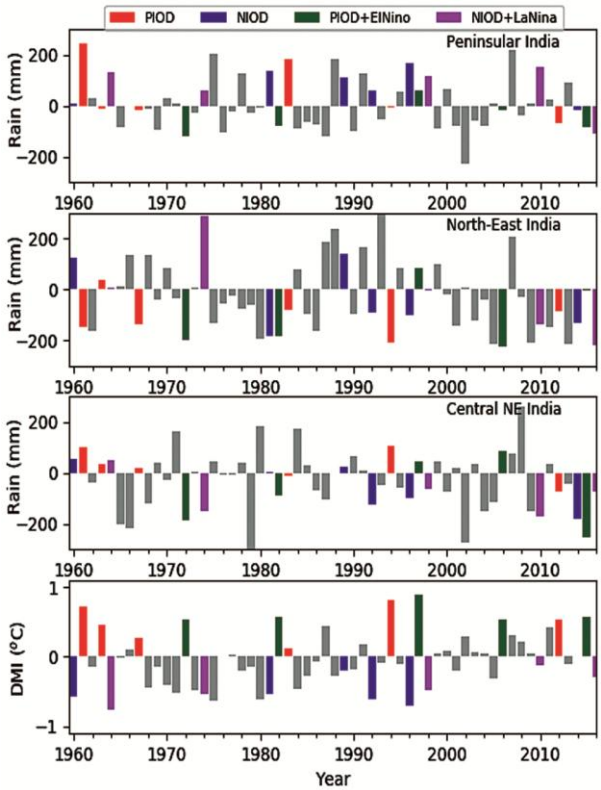

Fig. 10 — The southwest monsoon rainfall anomalies (mm) for Peninsular India, Northeast Indian and Central northeast India is plotted with DMI from 1960-2016

association with IOD events for the period 1960 to 2015. However, the results from only three regions (Central Northeast India, Northeast India & Peninsular India) are shown here due to their stronger relationship with IOD (Fig. 10).

The consensus from earlier studies is that PIODs are conducive for ISMR. During the pure PIOD years

(1961 and 1983) rainfall anomalies were highly positive in peninsular India. But in case of northeast region, all the IOD years contributes to negative rainfall anomalies, hence a deficit in rainfall. While taking the case of Central Northeast India, the rainfall anomaly is positive (excess rainfall) except for the year 2012.

The combination of PIOD and El-Nino resulted in a deficit rainfall for all the three regions in general. This is against the earlier findings that an IOD reduces the negative impact of El-Nino if they co-occur. However, in 1997 and 2006, rainfall anomaly was also found positive but with a lesser magnitude. The effect of PIOD-El-Nino has a lesser influence in Peninsular India as compared to other two regions.

The NIOD-La-Nina combination has resulted in excess rainfall (positive anomaly) for the Peninsular India and deficit rainfall (negative anomaly) for Central NE India. Their relationship is not strong for the North-East India (excess in 1974 and deficit in 2010).

Summary and Conclusions

The present study has analyzed the evolution of consecutive IOD events for the period 1994 to 1998. The study also compared the effect of positive and negative phases of IODs occurred independently and with El-Nino/La-Nina on various parameters in the Indian Ocean and also on the Indian Summer Monsoon Rainfall.

The evolution of 1994 strong PIOD is by easterly wind anomalies as a result of shoaling of the thermocline prior to the onset. The termination phase of this pure PIOD is influenced by positive NHF anomalies in the EB resulting in the termination surface signals. It is then transited through a normal year 1995 to a strong negative IOD event in 1996 because of the absence of easterlies and positive net heat gain in the EB. During the starting of the termination phase of the NIOD in 1996, a shoaling of thermocline can be seen. This shoaling get stronger by means of strong easterlies associated with El-Nino in the Pacific contributing to the generation of another strong PIOD in 1997. The termination of PIOD co-occurred with El-Nino is happened due to strong warm water advection from Pacific due to La-Nina event. This EB warming results in the deepening of thermocline in the EB and result in the generation of 1998 NIOD.

The study also includes the variability in the evolution features of IOD events that are occurred independently and co-occurred with the El-Nino and La-Nina. There are significant differences in the evolution, features and life span between these two types of IOD events. The life span and intensity was enhanced when a positive IOD is co-occurred with El-Nino. The El-Nino increases the positive SST anomalies in the western box, while the La-Nina in the eastern box of IOD. The upwelling features were studied by using D20 isotherm over vertical 2-D slice of temperature, which showed minor differences during the pure and co-occurred IOD events. The westward propagation of down-welling Rossby waves was seen in the year 1994 and 1997 because of the easterlies in eastern equatorial Indian Ocean during the generation of PIOD. During the year 1994 the Rossby wave propagation is only up to the central equatorial Indian Ocean. This wave is reaching in the western equatorial Indian Ocean only in the co-occurred year 1997 and maintained for the next year till the termination of El-Nino. So the generation of Rossby wave is influenced by the generation mechanism of PIOD and is maintained by strong El-Nino in 1997.

The positive IOD in general contributed to good rainfall in most of the years over Peninsular India. But for the northeast region, a PIOD is detrimental for ISMR. The central north east India had positive rainfall anomalies for almost all the years except 2012. The El-Nino and El-Nino-IOD co-occurred years are not conducive for positive rainfall anomalies for all the regions. During the year 1997, the rainfall anomalies were positive for all the three homogeneous regions of India even if it was a very strong El-Nino year, indicating the influence of PIOD on rainfall. The negative IOD events didn't showed positive correlation with ISMR. The results obtained in the present study are preliminary in nature as only limited samples (number of cases under different categories) were used for the analysis.

Supplementary Data

Supplementary data associated with this article is available in the electronic form at http://nopr.niscair.res.in/jinfo/ijms/IJMS_50(07)521-532_SupplData.pdf

Acknowledgements

The authors are thankful to the Department of Physical Oceanography, Cochin University of Science and Technology, for providing the facilities for carrying out the research work. Thanks to Dr. K. M. Santhosh and Dr. Phiros Shah for providing valuable information for the study. We are also thankful to the

CSIR-NIO, Goa for the support. Figures of this study were generated by using the ferret and python software. All the authors are thankful to the two anonymous reviewers for their helpful suggestions and comments in order to improve the paper.

Conflict of Interest

The authors declare that they have no conflict of interest.

Author Contributions

Conceptualization and design of the work: NA, MRR, RS & PKS; Data collection, analysis and interpretation, Software and writing – original draft: NA & PKS; and Supervision and writing – review, editing and final approval: MRR, RS & PKS.

References

1 Saji N H, Goswami B N, Vinayachandran P N & Yamagata T, A dipole mode in the tropical Indian Ocean, *Nature*, 40 (1) (1999) 360-363.

2 Webster P J, Moore A M, Loschnigg J P & Leben R R, Coupled ocean-atmosphere dynamics in the Indian Ocean during 1997-98, *Nature*, 401 (1999) 356-360. doi: https://doi.org/10.1038/43848

3 Hendon H, Indonesian rainfall variability: impacts of ENSO and local air – sea interaction, *J Clim*, 16 (2003) 1775–1790.

4 Vinayachandran P N, Saji N H & Yamagata T, Response of the equatorial Indian Ocean to an anomalous wind event during 1994, *Geo phy Res Let*, 26 (1999) 1613-1615.

5 Wang H, Murtugudde R & Kumar A, Evolution of Indian Ocean dipole and its forcing mechanisms in the absence of ENSO, *Clim Dyn*, 47 (2016) 2481–2500.

6 Rao S A, Luo J-J, Behera S K & Yamagata T, Generation and termination of Indian Ocean dipole events in 2003, 2006 and 2007, *Clim Dyn*, 33 (6) (2009) 751-756.

7 Nisa A, Ramesh Kumar M R, Sajeev R & Saji P K, Role of distinct flavours of IOD events on Indian summer monsoon, *Nat Hazards*, 82 (2016) 1317-1326. doi: https://doi.org/10.1007/s11069-016-2245-9

8 Lu Bo, Ren H-L, Scaife A A, Wu J, Dunstone N, *et al*., An extreme negative Indian Ocean Dipole event in 2016: dynamics and predictability, *Clim Dyn*, 89 (2018) 1432-0894, doi: https://doi.org/10.1007/s00382-017-3908-2

9 Ashok K, Guan Z & Yamagata T, Influence of the Indian Ocean dipole on the Australian winter rainfall, *Geophys Res Let*, 30 (15) (2003) 1821, doi: https://doi.org/10.1029/2003GL017926

10 Cai W, Pan A, Roemmich D, Cowan T & Guo X, Argo profiles a rare occurrence of three consecutive positive Indian Ocean Dipole events, 2006-2008, *Geophy Res Let*, 36 (2009) L08701. doi: https://doi.org/10.1029/2008GL037038

11 Wang G & Cai W, Two-year consecutive concurrences of positive Indian Ocean Dipole and Central Pacific El Niño preconditioned the 2019/2020 Australian "black summer" bushfires, *Geosci Lett*, **7** (19) (2020). doi: https://doi.org/10.1186/s40562-020-00168-2

12 Behera S K, Krishnan R & Yamagata T, Unusual ocean-atmosphere conditions in the tropical Indian Ocean during 1994, *Geophy Res Let*, 26 (1999) 3001-3004.

13 Saji N H, Dachao J & Vishnu T, A model for Super El-Niño's, *Nature Communications*, 2528, 9 (2018) 2041-1723, doi: https://doi.org/10.1038/s41467-018-04803-7

14 Shabbar A & Yu B, The 1998–2000 La Niña in the context of historically strong La Niña events, *J Geophy Res*, 114 (2009) D13105. doi: https://doi.org/10.1029/2008JD011185

15 Hong C C, Lu M M & Kanamitsu M, Temporal and spatial characteristics of positive and negative Indian Ocean dipole with and without ENSO, *J Geophy Res*, 113 (2008) 1-15, doi: https://doi.org/10.1029/2007JD009151

16 Kothawale D R & Rajeevan M, Monthly, Seasonal and Annual Rainfall Times for All India, Hmogenous Regions and Meteorological Subdivisions: 1971-2016. Research Report No. RR-138. Contribution from IITM, (http://www.tropmet.res.in/).

17 Kumar P, Vialard J, Lengaigne M, Murty V S N & McPhaden M J, TropFlux: Air-sea fluxes for the global tropical oceans-description and evaluation, *Clim Dyn*, 38 (2012) 1521-1543, doi: https://doi.org/10.1007/s00382-011-1115-0

18 *Andersson A, Fennig K, Klepp C, Bakan S, Graßl H, et al.*, The Hamburg Ocean Atmosphere Parameters and Fluxes from Satellite Data-HOAPS-3, *Earth Syst Sci Data*, 2 (2) (*2010)* 215-234.

19 Carton J A, Giese B S & Grodsky S A, Sea level rise and the warming of the oceans in the SODA ocean reanalysis, *J Geophys*, 110 (2005) C09006, doi: https://doi.org/10.1029/2004JC002817

20 Bentamy A, Queffeulou P, Quilfen Y & Katsaros K, Ocean surface wind fields estimated from satellite active and passive microwave instruments, *IEEE Trans Geosci Rem Sen*, 37 (1999) 2469-2486.

21 Ueda H & Matsumoto J, A possible triggering process of east–west asymmetric anomalies over the Indian Ocean in relation to 1997/98 El Nino, *J Meteorol Soc Jpn*, 78 (2000) 803–818.

22 Kajikawa Y, Yasunari T & Kawamura R, The role of local Hadley circulation over the western Pacific on the zonally asymmetric anomalies over the Indian Ocean, *J Meteorol Soc Jpn*, 81 (2001) 259–276, doi: https://doi.org/10.2151/jmsj.81.259